Journal of Statistical Physics, Vol. 94, Nos. 1/2, 1999

Universal Large-Deviation Function of the Kardar–Parisi–Zhang Equation in One Dimension

B. Derrida[1] **and C. Appert**[1]

Received July 10, 1998

Using the Bethe ansatz, we calculate the whole large-deviation function of the displacement of particles in the asymmetric simple exclusion process (ASEP) on a ring. When the size of the ring is large, the central part of this large deviation function takes a scaling form independent of the density of particles. We suggest that this scaling function found for the ASEP is universal and should be characteristic of all the systems described by the Kardar–Parisi–Zhang equation in $1+1$ dimension. Simulations done on two simple growth models are in reasonable agreement with this conjecture.

KEY WORDS: KPZ equation; Bethe ansatz; ASEP; Burgers equation; directed polymers; growth models; large-deviation function.

1. INTRODUCTION

The Kardar–Parisi–Zhang (KPZ) equation describes the large scale behavior of a number of systems ranging from growing interfaces to directed polymers in a random medium.[1–4] A main difficulty with the KPZ equation is that it is controlled, in all dimensions, by a strong disorder (or strong coupling) fixed point and tools are missing to calculate the exponents or other universal properties (scaling functions, amplitudes…).

In one dimension, the exponents are known[1, 2] but many properties, including the distribution function of the height of a growing interface, have so far been measured only in numerical simulations.

[1] Laboratoire de Physique Statistique (Laboratoire associé aux Universités Paris, 6, Paris 7 et au CNRS), Ecole Normale Supérieure, 75231 Paris Cedex 05, France; e-mail: appert@physique.ens.fr, derrida@physique.ens.fr.

0022-4715/99/0100-0001$16.00/0

In a recent paper,[5] it has been shown that for one particular model of the KPZ class, the asymmetric exclusion process (ASEP), the whole distribution of the displacement of particles could be calculated for a finite geometry by the Bethe ansatz. The displacement in the ASEP is equivalent, through a change of variables, to the height of a growing interface or to the free energy of a directed polymer in a random medium, so that the results of ref. 5 could be reinterpreted in several different contexts.

The expression obtained in ref. 5, which is rederived here in Section 2, gave only the probability distribution of the displacement in a certain range. Here we extend the results of ref. 5 and find analytic continuations which determine the probability distribution of the displacement everywhere. Although the existence of these continuations was doubtless, explicit expressions were so far missing. In Sections 4 and 5, we analyse the limit of a large system size. In its central part, the large deviation function takes a scaling form which we conjecture to be universal and characteristic of all the models belonging to the KPZ universality class (Section 4). In Section 5, we calculate the large deviation outside its central part and we show that the positive and the negative sides verify different scalings as argued in ref. 5. To test whether the central part of the large deviation function is universal, we use a Monte Carlo procedure to measure ratios of cumulants of the height for several models of growing interfaces. Although we were not able to determine these ratios with a high accuracy, the results presented in Section 6 are consistent with the claim that the ratio considered is universal.

2. BETHE ANSATZ FOR THE ASEP MODEL

In the ASEP, one considers a system of p particles moving on a ring of N sites. During every time interval dt, each particle jumps to the next site on its right with probability dt, if this site is empty. Otherwise, it does not move.

We are interested in the probability distribution $P(Y_t)$ of the total distance Y_t covered by *all* the particles between time 0 and t. It is known that the one dimensional ASEP is equivalent to a model of growing interface, so Y_t can also be considered as the space averaged height of a growing interface.[6–8]

The knowledge of the generating function $\langle e^{\alpha Y_t} \rangle$ determines the whole probability distribution $P(Y_t)$ of Y_t. In particular all the cumulants of Y_t are given by

$$\langle Y^n \rangle_c = \left. \frac{d^n \ln \langle e^{\alpha Y_t} \rangle}{d\alpha^n} \right|_{\alpha = 0} \tag{1}$$

It was shown in ref. 5 that for large t, the generating function $\langle e^{\alpha Y_t} \rangle$ increases exponentially with t

$$\langle e^{\alpha Y_t} \rangle \sim e^{\lambda_{\max}(\alpha)\, t} \tag{2}$$

where $\lambda_{\max}(\alpha)$ in (2) is the largest eigenvalue of a matrix

$$M(\alpha) = M_0 + e^{\alpha} M_1 \tag{3}$$

constructed from the transition matrix: $M_1(\mathscr{C}, \mathscr{C}')\, dt$ is the probability to go from a configuration $\mathscr{C}'$ to a configuration $\mathscr{C}$, during the infinitesimal time interval dt, by increasing Y_t by one. For the ASEP model, all possible moves increase Y_t by one, so M_1 is equal to the usual transition matrix except for the diagonal terms $M_1(\mathscr{C}, \mathscr{C}) = 0$. M_0 is a diagonal matrix representing the probability of escaping from a given configuration $\mathscr{C}$, i.e.,

$$M_0(\mathscr{C}, \mathscr{C}) = - \sum_{\mathscr{C}' \neq \mathscr{C}} M_1(\mathscr{C}', \mathscr{C}) \tag{4}$$

For large t, one expects the distribution $P(Y_t)$ to take the form

$$P(Y_t) \sim e^{tf(Y_t/t)} \tag{5}$$

Then the asymptotic behavior (2) of $\langle e^{\alpha Y_t} \rangle$ determines the large deviation function f

$$f(v) = \lim_{t \to \infty} \frac{\ln P(vt)}{t} \tag{6}$$

Indeed, writing that the generating function

$$\langle e^{\alpha Y_t} \rangle = \sum_{Y_t = 0}^{\infty} P(Y_t)\, e^{\alpha Y_t}$$

is dominated by the largest term $Y_t = vt$ of the sum gives from (2) and (5)

$$\max_v \left[f(v) + \alpha v \right] = \lambda_{\max}(\alpha)$$

This allows one to obtain the large deviation function f in the parametric form from the knowledge of $\lambda_{\max}(\alpha)$

$$\begin{aligned} v &= \frac{d\lambda_{\max}}{d\alpha} \\ f(v) &= \lambda_{\max}(\alpha) - \alpha \frac{d\lambda_{\max}}{d\alpha} \end{aligned} \tag{7}$$

The calculation of $\lambda_{\max}(\alpha)$ for arbitrary N and p can be done using the Bethe ansatz.[5] From the Bethe ansatz equations (a derivation is given in Appendix A), one can show that for any solution $\{y_j\}_{j=1 \text{ to } p}$ of the p equations

$$(1+y_j)^{-N} y_j^p = e^{\alpha N}(-1)^{(p-1)} \prod_{k=1}^{p} y_k \tag{8}$$

one gets an eigenvalue $\lambda(\alpha)$ of the matrix $M(\alpha)$

$$\lambda(\alpha) = -\sum_{j=1}^{p} \frac{y_j}{1+y_j} \tag{9}$$

It is in general not easy to decide which solution $\{y_j\}_{j=1 \text{ to } p}$ of (8) corresponds to the largest eigenvalue. Here, however, one can use the Perron Frobenius theorem because the matrix $M(\alpha)$ of (3) is irreductible and has all its off-diagonal elements positive or zero, so that by adding a matrix proportional to the identity matrix, it satisfies the conditions of the Person Frobenius theorem.[9] Thus, as α varies, the largest eigenvalue has no crossing and so $\lambda_{\max}(\alpha)$ can be followed continuously starting from $\lambda_{\max}(0)=0$ at $\alpha=0$ (at $\alpha=0$, $\lambda_{\max}(0)=0$ is just a consequence of the fact that $M(0)$ is a probability matrix).

Solving a system of p coupled non linear equations as in (8) is usually a non trivial task. To decouple these equations, we use the fact that (8) can be written as

$$y_j^p = B(1+y_j)^N \tag{10}$$

which is a polynomial equation for a single variable y_j. The price to pay is that one has to be sure that B coincides with the right hand side of (8), that is

$$B = e^{\alpha N}(-1)^{(p-1)} \prod_{k=1}^{p} y_k \tag{11}$$

In practice we use (11) to calculate α as a function of B

$$\alpha = \frac{1}{N} \ln \left[B(-1)^{(p-1)} \Big/ \prod_{k=1}^{p} y_k \right] \tag{12}$$

and we take the solution $\{y_j\}_{j=1 \text{ to } p}$ of (10) obtained by continuity from the solution

$$y_j \simeq B^{1/p} e^{2i\pi j/p} \qquad \text{for} \quad 1 \leqslant j \leqslant p \tag{13}$$

for small positive B. In this way, $\lambda_{\max}(\alpha)$ and α are both functions of B and so this gives $\lambda_{\max}$ as a function of α in a parametric form. This procedure which is reproduced in appendix B leads to the following expression of $\lambda_{\max}(\alpha)$ already given in ref. 5

$$\lambda_{\max}(\alpha) = -p \sum_{q=1}^{\infty} B^q \frac{(Nq-2)!}{(pq)!\,(Nq-pq-1)!} \tag{14}$$

$$\alpha = -\sum_{q=1}^{\infty} B^q \frac{(Nq-1)!}{(pq)!\,(Nq-pq)!} \tag{15}$$

valid for arbitrary N and p.

Clearly when $B \to 0$, both $\lambda_{\max}(\alpha)$ and α vanish and this justifies choice (13) for the largest eigenvalue $\lambda_{\max}$ of $M(\alpha)$ when $\alpha \to 0$. When B varies, the eigenvalue given by (14)–(15) changes continuously with B. As the Perron Frobenius theorem insures that the largest eigenvalue of $M(\alpha)$ has no crossing, expressions (14)–(15) keep giving the largest eigenvalue $\lambda_{\max}(\alpha)$ as long as the series converge.

The radius of convergence of (14)–(15) is

$$B_c = \frac{p^p (N-p)^{(N-p)}}{N^N} \tag{16}$$

and therefore (14)–(15) give $\lambda_{\max}(\alpha)$ only for

$$\alpha_- < \alpha < \alpha_+ \tag{17}$$

where

$$\alpha_- = -\sum_{q=1}^{\infty} (B_c)^q \frac{(Nq-1)!}{(qp)!\,(qN-qp)!} \tag{18}$$

$$\alpha_+ = -\sum_{q=1}^{\infty} (-B_c)^q \frac{(Nq-1)!}{(qp)!\,(qN-qp)!} \tag{19}$$

It is easy to check from (14)–(15) that $\lambda_{\max}$ and α are singular functions of B as $B \to B_c$. However from the Perron Frobenius theorem, we know

that $\lambda_{\max}(\alpha)$ as a function of α has no singularity for any real α and therefore is *not singular* as $\alpha \to \alpha_{\pm}$. This means the function $\lambda_{\max}(\alpha)$ can be analytically continued beyond the region (17). We will give in the next section two different expressions of $\lambda_{\max}(\alpha)$ valid in the two regions $\alpha < \alpha_-$ and $\alpha > \alpha_+$.

To illustrate the fact that the singularities in B of $\lambda_{\max}$ and of α disappear when one considers $\lambda_{\max}$ as a function of α, it is instructive to consider the simple example $p=1$ and $N=2$, for which the two series (14)–(15) can be summed easily. One finds the following expressions valid for $B < B_c = 1/4$

$$\lambda_{\max}(\alpha) = -\frac{1}{2}(1-(1-4B)^{1/2}) \tag{20}$$

$$\alpha = \ln\left(\frac{1+(1-4B)^{1/2}}{2}\right) \tag{21}$$

which both have a singularity as $B \to B_c$. In this simple example, it is however clear that

$$\lambda_{\max}(\alpha) = e^{\alpha} - 1 \tag{22}$$

remains regular even when $\alpha \to \alpha_{\pm}$.

3. ANALYTICAL CONTINUATION OF $\lambda_{\max}(\alpha)$ OUTSIDE THE REGION $\alpha_- < \alpha < \alpha_+$

In this section, we present two alternative expressions of $\lambda_{\max}(\alpha)$ which give the analytic continuation of (14)–(15) outside the region (17).

For $\alpha < \alpha_-$ we choose the solution $\{y_j\}_{j=1 \text{ to } p}$ of the equation (10) obtained by continuity from the solution

$$\begin{aligned} y_j &\simeq B^{1/p} e^{2i\pi j/p} \qquad \text{for} \quad 1 \leqslant j \leqslant p-1 \\ y_p &\simeq B^{-1/(N-p)} \end{aligned} \tag{23}$$

for small positive B. For $0 < B < B_c$, if we denote by $a(B)$ and $b(B)$ the two positive real roots y_j of (10) with the convention that $a(B) \leqslant b(B)$, the only difference between choices (13) and (23) is that y_p which was equal to $a(B)$ in (13) has now become $b(B)$ in (23). Therefore the expression of the eigenvalue $\lambda(\alpha)$ for choice (23) is almost identical to the expression (14)–(15)

except that we have replaced the contribution of $a(B)$ by the contribution of $b(B)$ in (9), (B7). This leads to

$$\lambda_{\max}(\alpha) = \frac{a(B)}{1+a(B)} - \frac{b(B)}{1+b(B)} - p \sum_{q=1}^{\infty} B^q \frac{(Nq-2)!}{(qp)!\,(qN-qp-1)!} \tag{24}$$

$$\alpha = \frac{\ln[1+a(B)] - \ln[1+b(B)]}{p} - \sum_{q=1}^{\infty} B^q \frac{(Nq-1)!}{(qp)!\,(qN-qp)!} \tag{25}$$

The fact that (24)–(25) is still the largest eigenvalue of $M(\alpha)$ follows from the fact that as $B \to B_c$, the eigenvalues given by (24)–(25) and (14)–(15) become identical (because (10) has a double root $a(B_c) = b(B_c)$ when $B = B_c$) and from the known fact that there is no crossing of the largest eigenvalue. For small B, the contributions of $a(B)$ and $b(B)$ in (24)–(25) dominate the sums and

$$\lambda_{\max}(\alpha) \simeq -1 + B^{1/p} + B^{1/(N-p)} + \cdots$$

$$\alpha \simeq \frac{\ln B}{p(N-p)} + \cdots$$

so that as B varies between 0 and B_c, α takes all possible real values between $-\infty$ and α_-.

The range $\alpha > \alpha_+$ is given by the analytic continuation of (14)–(15) to the range $B < -B_c$. When B becomes negative and very large, the N roots y_j of (10) approach -1 on a circle of radius $|B|^{-1/N}$. The solution we select (to give the largest eigenvalue) is such that for large negative B

$$y_j \simeq -1 + |B|^{-1/N} e^{i\pi(p+1-2j)/N} \qquad \text{for} \quad 1 \leqslant j \leqslant p \tag{26}$$

and is B varies from $-\infty$ to $-B_c$, the eigenvalue obtained by continuity from this solution is (see Appendix B)

$$\lambda_{\max}(\alpha) = \left(\frac{p}{N} - 1\right) \sum_{k=-1}^{\infty} \frac{\Gamma((pk/N)+1)}{(k+1)!\,\Gamma((pk/N)-k+1)} \frac{1}{|B|^{k/N}} (-)^k \frac{\sin(pk\pi/N)}{\sin(k\pi/N)} \tag{27}$$

$$\alpha = \frac{1}{N}\ln(|B|) - \frac{1}{N} \sum_{k=1}^{\infty} \frac{\Gamma(pk/N)}{k!\,\Gamma((pk/N)-k+1)} \frac{1}{|B|^{k/N}} (-)^k \frac{\sin(pk\pi/N)}{\sin(k\pi/N)} \tag{28}$$

To illustrate that (24)–(25) and (27)–(28) do give the analytic continuation of (14)–(15), one can look again at the example $p=1$ and $N=2$. In this case,

$$a(B)=\frac{1}{2B}(1-2B-(1-4B)^{1/2})$$

$$b(B)=\frac{1}{2B}(1-2B+(1-4B)^{1/2})$$

and the analytic continuation (24)–(25) gives

$$\lambda(\alpha)=-\frac{1}{2}(1+(1-4B)^{1/2})$$

$$\alpha=\ln\left(\frac{1-(1-4B)^{1/2}}{2}\right)$$

instead of (20)–(21). As B varies between 0 and 1/4, one recovers (22) for the range $\alpha<\alpha_-=-\ln 2$.

It is even simpler to check in this example that (27)–(28) is the right analytic continuation for $\alpha>\alpha_+$, because it simply gives, when $p=1$ and $N=2$, the expansion of (20)–(21) for large negative B.

4. SCALING OF THE LARGE DEVIATION FUNCTION

The expression (14)–(15) is valid in the range $\alpha_-<\alpha<\alpha_+$ which includes $\alpha=0$ and therefore describes the large deviation function $f(v)$ in the infinite time limit for v close to its average value

$$\frac{\langle Y_t\rangle}{t}=\frac{p(N-p)}{N-1}$$

When $N\to\infty$ keeping the ratio $p/N=\rho$ fixed, one can show using Stirling's formula that (14)–(15) takes the scaling form[5]

$$\lambda_{\max}(\alpha)-\alpha N\rho(1-\rho)=\sqrt{\frac{\rho(1-\rho)}{2\pi N^3}}\,G(\alpha\sqrt{2\pi\rho(1-\rho)\,N^3}) \qquad (29)$$

where the scaling function G is independent of the parameters of the model (here N and ρ) and has the following parametric form

$$\beta = -\sum_{q=1}^{\infty} (-C)^q q^{-3/2} \tag{30}$$

$$G(\beta) = -\sum_{q=1}^{\infty} (-C)^q q^{-5/2} \tag{31}$$

where $C = -B/B_c$. Up to a simple factor, these expressions are identical to those of the pressure (for $G(\beta)$) and the density (for β) of an ideal Fermi gas when $C > 0$ and of an ideal Bose gas when $C < 0$ (in fact $\ln |C|$ is just the chemical potential).

As C crosses the value 1, the function $G(\beta)$ can be analytically continued easily using the analogy with the Fermi gas for which it is known that there is no phase transition as the chemical potential C varies. One can for example replace (30)–(31) by

$$\beta = \frac{2}{\sqrt{\pi}} \int_0^{\infty} \varepsilon^{1/2} \frac{Ce^{-\varepsilon}\, d\varepsilon}{1 + Ce^{-\varepsilon}} \tag{32}$$

$$G(\beta) = \frac{4}{3\sqrt{\pi}} \int_0^{\infty} \varepsilon^{3/2} \frac{Ce^{-\varepsilon}\, d\varepsilon}{1 + Ce^{-\varepsilon}} \tag{33}$$

These two expressions coincide with (30)–(31) in the range $-1 < C < 1$ and so provide an analytic continuation to the range $C > 1$.

As C approaches -1, one could expect to observe the Bose–Einstein condensation (which would mean that for $\beta < \beta_- \equiv -\sum_{q \geqslant 1} q^{-3/2}$, the function $G(\beta)$ would remain constant taking the value $-\sum_{q \geqslant 1} q^{-5/2}$). Instead, as the function $G(\beta)$ can be analytically continued beyond β_-, one finds that the analytic continuation is given by

$$\beta = -4\sqrt{\pi}\, [-\ln(-C)]^{1/2} - \sum_{q=1}^{\infty} (-C)^q q^{-3/2} \tag{34}$$

$$G(\beta) = \tfrac{8}{3}\sqrt{\pi}\, [-\ln(-C)]^{3/2} - \sum_{q=1}^{\infty} (-C)^q q^{-5/2} \tag{35}$$

and as C varies between 0 and -1, this gives the function $G(\beta)$ for all $\beta < \beta_-$. There are several ways of deriving (34)–(35). One of them is to start from (24)–(25) and to choose $B = -CB_c$. When C is negative and of

order 1 and N is large, the two positive roots $a(B)$ and $b(B)$ of (10) (obtained by taking the ln of (10)) are given by

$$a(B) = \frac{\rho}{1-\rho}\left[1 - \left(\frac{-2\ln(-C)}{\rho(1-\rho)\,N}\right)^{1/2} + O\left(\frac{1}{N^{3/2}}\right)\right]$$

$$b(B) = \frac{\rho}{1-\rho}\left[1 + \left(\frac{-2\ln(-C)}{\rho(1-\rho)\,N}\right)^{1/2} + O\left(\frac{1}{N^{3/2}}\right)\right]$$

and one finds, using (24)–(25) and (29) for large N, that $G(\beta)$ is given by (34)–(35). Alternatively, one can try to find directly the analytic continuation of expressions (30)–(31) to $\beta < \beta_-$ and this leads to the same expression (34)–(35).

The behavior of $G(\beta)$ for small or large β can be easily extracted from the three expressions (30)–(31), (32)–(33), (34)–(35). By eliminating C (for $|C|$ small) in the expansions (30)–(31), one finds that for small β

$$G(\beta) = \beta + \frac{\sqrt{2}}{8}\beta^2 + \frac{27-16\sqrt{3}}{216}\beta^3 + \frac{18+15\sqrt{2}-16\sqrt{6}}{192}\beta^4 + O(\beta^5) \quad (36)$$

By looking at the large C behavior of (32)–(33), one finds that $\beta \simeq 4(\ln C)^{3/2}/(3\sqrt{\pi})$ and $G(\beta) \simeq 8(\ln C)^{5/2}/(15\sqrt{\pi})$ and this gives for $\beta \to \infty$

$$G(\beta) \simeq \frac{1}{5}\left(\frac{9\pi}{2}\right)^{1/3}\beta^{5/3} \quad (37)$$

Lastly, by choosing C small and negative one obtains from (34)–(35) that when $\beta \to -\infty$

$$G(\beta) \simeq -\frac{\beta^3}{24\pi} \quad (38)$$

From (7) and (29), it follows that $f(v)$ defined by (6) has also a scaling form

$$v = N\rho(1-\rho) + \rho(1-\rho)\frac{dG(\beta)}{d\beta} \quad (39)$$

$$f(v) = \sqrt{\frac{\rho(1-\rho)}{2\pi N^3}}\left[G(\beta) - \beta\frac{dG(\beta)}{d\beta}\right] \quad (40)$$

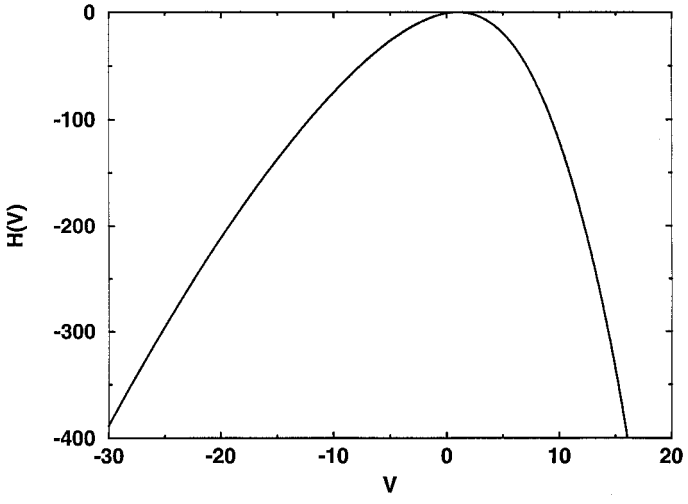

Fig. 1. Scaling form $H(V)$ of the large deviation function given by (30)–(35), (42), (43).

This shows that for large N and arbitrary ρ, all the large deviation functions $f(v)$, once properly rescaled, have the same shape

$$f(v) = \sqrt{\frac{\rho(1-\rho)}{\pi N^3}}\, H\left(\frac{v - N\rho(1-\rho)}{\rho(1-\rho)}\right) \tag{41}$$

where the scaling function $H(V)$ is directly obtained from the function $G(\beta)$ as

$$V = G'(\beta) \tag{42}$$

$$H(V) = \frac{1}{\sqrt{2}}\left[\, G(\beta) - \beta \frac{dG(\beta)}{d\beta}\right] \tag{43}$$

As we know from (30)–(35) the function $G(\beta)$ for all β, this determines the scaling function $H(V)$ for all V and its shape is shown in Fig. 1.

The knowledge (36)–(38) of $G(\beta)$ for small and large β gives also the limiting behaviors of $H(V)$ for small and large V

$$H(V) = -(V-1)^2 + O(V-1)^3 \qquad \text{for} \quad |V-1| \ll 1 \tag{44}$$

$$H(V) \simeq -[2\sqrt{3}/(5\sqrt{\pi})]\, V^{5/2} \qquad \text{for} \quad V \to +\infty \tag{45}$$

$$H(V) \simeq -[4\sqrt{\pi}/3]\, |V|^{3/2} \qquad \text{for} \quad V \to -\infty \tag{46}$$

These results were already presented in ref. 5 except for mistakes or misprints in (25), (26) and (31) of ref. 5 which have been now corrected in (35), (38), (46).

As the scaling form $H(V)$ is independent of N and ρ, one can conjecture, in the spirit of Krug,[10] that it is universal and that one should recover it for all models belonging to the KPZ universality class.

5. LARGE DEVIATION FUNCTION OUTSIDE THE SCALING REGION

In the previous section, we have seen that $f(v)$ has the scaling form (41) for large N as long as the difference $v - N\rho(1-\rho)$ is of order 1, i.e. for deviations of order 1 of the Y_t/t from its average.

One can also try to calculate $f(v)$ when the difference $v - N\rho(1-\rho)$ is of order N. In ref. 5, it was argued that depending on the sign of this difference, $f(v)$ for large N has two possible forms

$$f(v) \simeq N H_+(v/N) \qquad \text{for} \quad \frac{v}{N} - \rho(1-\rho) > 0 \tag{47}$$

$$f(v) \simeq H_-(v/N) \qquad \text{for} \quad \frac{v}{N} - \rho(1-\rho) < 0 \tag{48}$$

With the help of the explicit expressions of Section 3, we can now justify this claim and give explicit expressions of the functions H_+ and H_-.

Let us first consider the case $\alpha < \alpha_-$ and $B \ll B_c$ where the parametric form (24)–(25) can be used. In this case, both α and the difference $\lambda_{\max}(\alpha) - \alpha N\rho(1-\rho)$ are dominated by the contributions of the two roots $a(B)$ and $b(B)$. This means that (24)–(25) can be replaced by

$$\lambda_{\max}(\alpha) \simeq \frac{a(B)}{1+a(B)} - \frac{b(B)}{1+b(B)} \tag{49}$$

$$\alpha \simeq \frac{\ln[1+a(B)] - \ln[1+b(B)]}{p} \tag{50}$$

Using the fact that $a(B)$ and $b(B)$ satisfy (10), one can see that

$$\left(\frac{a}{b}\right)^p = \left(\frac{1+a}{1+b}\right)^N \tag{51}$$

and eliminating $b(B)$ between (50) and (51) yields in terms of α

$$a(B) = \frac{1 - e^{\alpha p}}{e^{\alpha(p-N)} - 1} \tag{52}$$

and

$$\lambda_{\max}(\alpha) \simeq \frac{-(1 - e^{\alpha\rho N})(1 - e^{\alpha(1-\rho)N})}{(1 - e^{\alpha N})} \tag{53}$$

As a consequence, we see that in the whole range where α is of order $1/N$, the large deviation function $f(v)$ in the large N limit obtained from (53) by use of (7) scales as

$$f(v) \simeq H_-\left(\frac{v}{N}\right) \tag{54}$$

where the function $H_-(W)$ is given in a parametric form by

$$W = \frac{dF(\eta)}{d\eta} \qquad \text{and} \qquad H_-(W) = F(\eta) - \eta \frac{dF(\eta)}{d\eta}$$

and the function $F(\eta)$ by

$$F(\eta) = -\frac{(1 - e^{\rho\eta})(1 - e^{(1-\rho)\eta})}{1 - e^{\eta}}$$

The fact that $F(\eta) \to -1$ as $\eta \to -\infty$ and that $F(\eta) \simeq \rho(1-\rho)\eta - \rho^2(1-\rho)^2\eta^3/12$ as $\eta \to 0$ implies the following behaviors of $H_-(W)$

$$H_-(W) \to -1 \qquad \text{for} \quad W \to 0 \tag{55}$$

$$H_-(W) \simeq -\frac{4[\rho(1-\rho) - W]^{3/2}}{3\rho(1-\rho)} \qquad \text{for} \quad 0 < \rho(1-\rho) - W \ll 1 \tag{56}$$

These two limiting behaviors are expected. In the limit $W \to 0$, the easiest way to achieve the fact that no particle moves is that a single particle does not move (and this particle prevents of course all the other particles from moving). When $v \to N\rho(1-\rho)$ we see by comparing (56) with the results of the previous section that the expression (54), (56) of $f(v)$ for $0 < (N\rho(1-\rho) - v)/N \ll 1$ obtained here agrees with the expression (41), (46) of $f(v)$ for $N\rho(1-\rho) - v \gg 1$ and so this common expression is certainly correct in the whole range $1 \ll N\rho(1-\rho) - v \ll N$.

Let us now consider the expression (27)–(28) valid for $\alpha > \alpha_+$. In the large N limit, using the identity $\Gamma(z)\,\Gamma(1-z) = \pi/(\sin \pi z)$, they become

$$\alpha = -\ln(\gamma) + \sum_{k=1}^{\infty} \frac{\Gamma(\rho k)\,\Gamma(k-\rho k)}{k!} \frac{(\sin k\rho\pi)^2}{k\pi^2} \gamma^k$$

and

$$\lambda_{\max}(\alpha) = N(1-\rho)\left[\frac{\sin \rho\pi}{\pi(1-\rho)} \frac{1}{\gamma} - \rho + \sum_{k=1}^{\infty} \frac{\Gamma(\rho k+1)\,\Gamma(k-\rho k)}{(k+1)!} \frac{(\sin k\rho\pi)^2}{k\pi^2} \gamma^k \right]$$

where $\gamma = |B|^{-1/N}$. Under this form it is easy to see, using (7), that whenever $v - N\rho(1-\rho)$ is positive and of order N

$$f(v) \simeq N H_+\left(\frac{v}{N}\right) \tag{57}$$

Taking the limit $\gamma \to 0$ or $\gamma \to \rho^{-\rho}(1-\rho)^{-(1-\rho)}$ leads to the following limiting behaviors for H_+

$$H_+(W) \simeq -W \ln W \qquad \text{for} \quad W \to \infty \tag{58}$$

$$H_+(W) \simeq -\frac{2\sqrt{3}\,[W - \rho(1-\rho)]^{5/2}}{5\pi(\rho(1-\rho))^2} \qquad \text{for} \quad 0 < W - \rho(1-\rho) \ll 1 \tag{59}$$

and here again the expression of $f(v)$ (57), (59) derived for $0 < (v - \rho(1-\rho)\,N)/N \ll 1$ coincides with (7), (45) derived for $v - N\rho(1-\rho) \gg 1$, so that this common expression is valid for the whole range $1 \ll v - N\rho(1-\rho) \ll N$.

6. UNIVERSAL RATIO OF CUMULANTS

It is not easy to measure the large deviation function $f(v)$ defined by (6) in a Monte Carlo simulation because $f(v)$ corresponds to a large t limit where the probability $P(vt)$ is exponentially small. If the time t used to measure $P(Y_t)$ is too small, the large t limit is not reached. On the other hand, if t is large enough, the statistics are often very bad because there are too few events.

The scaling form (44)–(46) is even harder to confirm numerically because on top of making the simulations for large enough t, the system

size N has also to be large enough. Moreover because the scaling form (44)–(46) is valid only for $v - N\rho(1-\rho)$ of order 1, it is hard to decide in simulations done for finite and relatively small N where $v - N\rho(1-\rho) \sim 1$ is supposed to hold.

In order to test the universality of the scaling form of Section 4, we have measured the following ratio of cumulants of Y_t

$$R_t = \frac{[\langle Y_t^3 \rangle_c]^2}{\langle Y_t^2 \rangle_c \langle Y_t^4 \rangle_c} \tag{60}$$

According to (1), (2), (29), (26), for N sufficiently large,

$$\lim_{t \to \infty} \frac{\langle Y^2 \rangle - \langle Y \rangle^2}{t} \simeq N^{3/2} [\rho(1-\rho)]^{3/2} \frac{\sqrt{\pi}}{2} \tag{61}$$

$$\lim_{t \to \infty} \frac{\langle Y^3 \rangle - 3\langle Y^2 \rangle \langle Y \rangle + 2\langle Y \rangle^3}{t} \simeq N^3 [\rho(1-\rho)]^2 \left(\frac{3}{2} - \frac{8}{3^{3/2}} \right) \pi \tag{62}$$

$$\lim_{t \to \infty} \frac{\langle Y^4 \rangle - 3\langle Y^2 \rangle^2 - 4\langle Y^3 \rangle \langle Y \rangle + 12\langle Y^2 \rangle \langle Y \rangle^2 - 6\langle Y \rangle^4}{t} \simeq N^{9/2} [\rho(1-\rho)]^{5/2} \left(\frac{15}{2} + \frac{9}{2^{1/2}} - \frac{24}{3^{1/2}} \right) \pi^{3/2} \tag{63}$$

and for large enough N and t (one has to take the limit $t \to \infty$ first), the ratio R_t is independent of N and ρ and becomes a number characteristic of the scaling function $G(\beta)$

$$\lim_{t \to \infty} R_t = \frac{[G^{(3)}(0)]^2}{G''(0)\, G^{(4)}(0)} = 2 \frac{(3/2 - 8/3^{3/2})^2}{(15/2 + 9/\sqrt{2} - 24/\sqrt{3})} \simeq 0.41517\ldots \tag{64}$$

As we expect the scaling function $G(\beta)$ to be universal, the ratio R_t in the limit $t \to \infty$ should be the same for all the growth models belonging to the KPZ universality class. In this section we perform Monte Carlo simulations for several growth models including the ASEP to measure the ratio R_t and to test the validity of (64).

6.1. The ASEP

In Section 2, we gave the exact expression (14)–(15) of $\lambda(\alpha)$ for the ASEP in its continuous time version. Therefore we know from (1) and (60) the exact values of $\lim_{t\to\infty} R_t$ for all N and p (see Table 1). Simulations are always done with a discrete time. This has the effect of changing the values of R_t (for finite N and p). We are now going to see that one can also extract from (14)–(15) the exact values of $\lim_{t\to\infty} R_t$ for all N and p for discrete dynamics.

In our simulations described below, at each time step $\Delta t = 1/p$, we choose at random one particle among the p particles. We move it to the next site on its right if this site is empty and leave it unchanged otherwise. As in (2), one expects, in the discrete time version, the generating function of Y_t to grow exponentially for large t

$$\langle e^{\alpha Y_t} \rangle \sim e^{\mu(\alpha) t}$$

It is easy to relate the eigenvalues $\lambda(\alpha)$ and $\mu(\alpha)$ for the continuous and discrete time versions. In the continuous case, the evolution equation for the probability $Q_t(\mathscr{C})$ of having a configuration $\mathscr{C}$ of the particles on the ring at time t is

$$\frac{d}{dt} Q_t(\mathscr{C}) = \sum_{\mathscr{C}'} [M_0(\mathscr{C}, \mathscr{C}') + M_1(\mathscr{C}, \mathscr{C}')] Q_t(\mathscr{C}')$$

Table 1. Exact Values of $\lim_{t\to\infty} R_t$ for Various System Sizes for Continuous or Discrete Time Versions of the ASEP, for a Density $\rho = p/N = 1/2$

N	p	Continuous time	Discrete time
10	5	0.00028554	0.64059215
20	10	0.20750073	0.48515157
40	20	0.32450840	0.45703829
80	40	0.37306198	0.44690072
160	80	0.39488281	0.44028506
320	160	0.40521261	0.43481181
640	320	0.41023726	0.43019816
1280	640	0.41271517	0.42643972
2560	1280	0.41394560	0.42348782
5120	2560	0.41455869	0.42123614
10240	5120	0.41486471	0.41955540
$+\infty$	$+\infty$	0.41517037	0.41517037

while for the discrete time version it reads

$$Q_{t+\Delta t}(\mathscr{C}) = Q_t(\mathscr{C}) + \frac{1}{p} \sum_{\mathscr{C}'} [M_0(\mathscr{C}, \mathscr{C}') + M_1(\mathscr{C}, \mathscr{C}')] \, Q_t(\mathscr{C}')$$

where the matrices M_0 and M_1 have already been introduced in (3). This shows that

$$\mu(\alpha) = p \ln \left[1 + \frac{\lambda(\alpha)}{p} \right] \tag{65}$$

The cumulants in the discrete case are obtained from the derivatives of the eigenvalue $\mu(\alpha)$ as in (1), i.e.,

$$\lim_{t \to \infty} \frac{\langle Y^n \rangle_c}{t} = \frac{d^n \mu(\alpha)}{d\alpha^n} \bigg|_{\alpha = 0} \tag{66}$$

and therefore the knowledge of $\mu(\alpha)$ through (14), (15), (65) gives the large t limit of R_t for all system sizes. In Table 1, we give the exact limiting values $\lim_{t \to \infty} R_t$ for different system sizes, both for the continuous and discrete time versions. In the infinite system size limit, $\lim_{t \to \infty} R_t$ converges towards the same value (64) for both the continuous and discrete versions.

In numerical simulations, we can compute the cumulant ratio R_t only for finite t and in the long time limit this ratio R_t should converge towards the values given in Table 1 for each size N.

We show in Figure 2 the ratios R_t versus t measured in a Monte Carlo simulation for three system sizes $N = 10$, 20 and 40 at density $p/N = 1/2$. We averaged over 5×10^{10} time steps per particle, so that the total number of updates was $5p \times 10^{10}$. Despite these rather long simulations, the fluctuations are visible. They are consistent with the limiting values expected in Table 1 (shown as dashed lines) although for $N = 40$, the measured value is systematically below at a distance of about one or two error bars. Error bars were estimated from 50 independent subsets of the data (each corresponding to 10^9 time steps). Our first simulations (not shown here) gave results which were in strong disagreement with the exact expected values of Table 1. We took a "better random number generator" and the results were greatly improved but we cannot exclude that our simulation results shown in Figure 2 are not biased at all by the random number generator. We tried to simulate larger sizes $N = 80, 160, \ldots$ but the long time limit of R_t takes longer and longer to reach[11, 12] as N increases and we were not convinced that our data gave a good estimate of this long time limit.

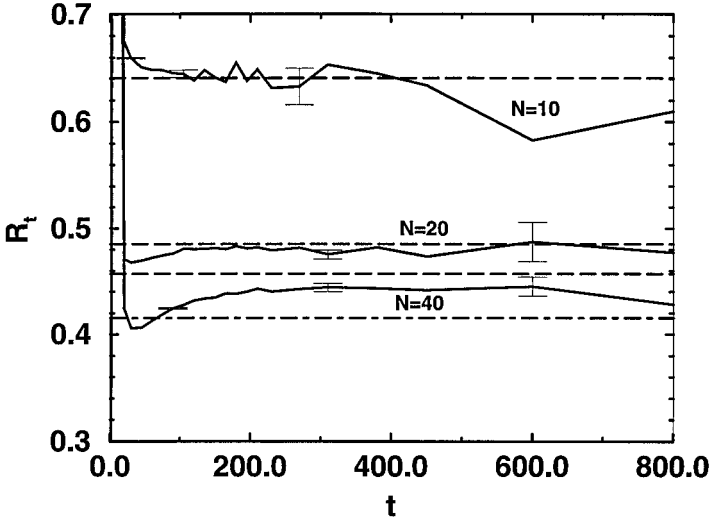

Fig. 2. Ratio R_t versus t for different system sizes, measured for the ASEP model. The density of particles is $\rho = p/N = 1/2$. The horizontal dashed lines give the long time limits of R_t for each system size and the horizontal semi dashed line indicates the expected asymptotic value 0.41517... predicted in (64) (large N and t with the limit $t \to \infty$ first).

6.2. Other Growth Models

We used also the Monte Carlo method to measure the ratio R_t for two other growth models which are expected to belong to the KPZ universality class.[1] For both models, a configuration at time t is specified by the height $h_i(t)$ at site i on a one dimensional lattice of L sites with periodic boundary conditions (so that sites $L+i$ and i are identified).

In the first model (that we will call a *brick model*), at each time step $\Delta t = 1/L$, a brick of width 2 is dropped at a random location (i_0, i_0+1) and the new heights at these sites become

$$h_{t+\Delta t}(i_0) = h_{t+\Delta t}(i_0+1) = \max[h_t(i_0), h_t(i_0+1)] + 1 \tag{67}$$

All the other heights $h(i)$ remain unchanged for $i \neq i_0, i_0+1$.

In the second model (called *ballistic deposition*),[1, 6] at each time step $\Delta t = 1/L$, a sticking square is dropped at a random location i_0 and it sticks to the first square it touches on the existing surface. Therefore, at each time step, all heights $h(i)$ remain unchanged except for the height $h(i_0)$ which becomes

$$h_{t+\Delta t}(i_0) = \max[h_t(i_0)+1, h_t(i_0-1), h_t(i_0+1)] \tag{68}$$

For both models, Y_t is defined by

$$Y_t = \sum_{i=1}^{L} h_t(i) \tag{69}$$

For these two growth models, we have measured (see Figs. 3 and 4) the ratio R_t for $L = 20, 40, 80, 160, 320$. The cumulants of Y_t were averaged over a time ranging from 10^8 for the largest size $L = 320$ up to 10^{10} for $L = 20$. As for the ASEP, the fluctuations are still visible and it is clear that as L increases, R_t takes longer and longer to reach its asymptotic value, making the simulation of larger systems problematic. For these two growth models, the convergence as L increases to the value 0.41517... predicted in (64) seems to be better than for the ASEP model (see Figs. 3 and 4). We have however to admit that the results are less convincing than what we hoped when we started these simulations. In particular the distance between successive curves corresponding to different L does not seem to decrease when L increases as it should for the curves to accumulate to the asymptotic value when the system size increases. The fact that the accumulation is not visible here can be explained as follows. We have observed that the ratio R_∞ is not a monotonous function of the system size but reaches a maximum around $L = 20$ (this is not shown on the Figs. 3

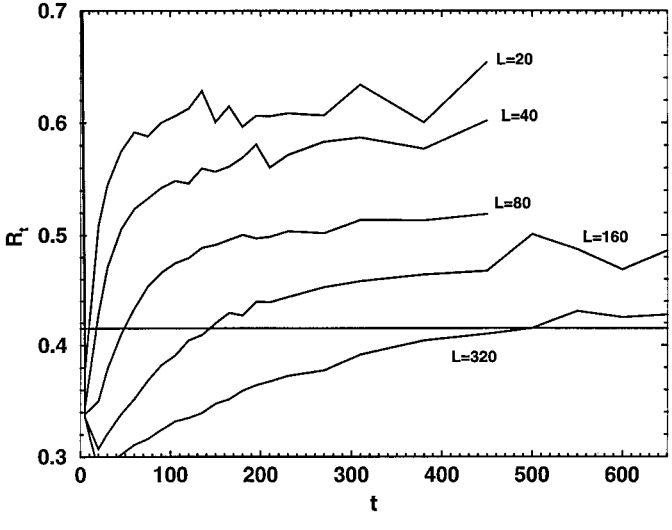

Fig. 3. Ratio R_t for the fist growth model (brick model). The horizontal line indicates the expected asymptotic value 0.41517...

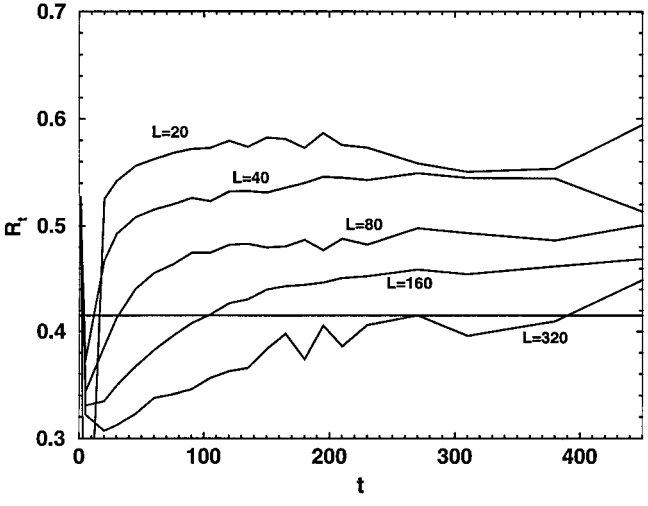

Fig. 4. Ratio R_t for the second growth model (ballistic deposition). The horizontal line indicates the expected asymptotic value 0.41517...

and 4 to keep them readable). We think that this is why curves seem more or less equally spaced for the system sizes we were able to simulate.

7. CONCLUSION

In this work, we have calculated exactly the large deviation function of the displacement of the ASEP (asymmetric simple exclusion process) by using an extension of the Bethe ansatz of Gwa and Spohn.[11, 12] The central part of the large deviation function had already been obtained recently in ref. 5 and here we have obtained explicit expressions of the large deviation function (or more precisely of its generating function in the large t limit) valid everywhere. The analytical continuations of Section 3 have allowed us to obtain explicit expressions for the tails of the distribution.

For the ASEP, when the system size is large, the central part of the large deviation function takes a scaling form (Section 4) independent of the microscopic details of the model (here it is independent of the density of particles), suggesting that this scaling function is universal and should be visible for all growth models belonging to the KPZ class.

In Section 6, we tried to check this conjecture by measuring a ratio of cumulants of the height for a few growth models by a Monte Carlo method. For the ASEP as well that the two other growth models we considered, our numerical results look consistent with the conjectured universal value of the ratio of cumulants. The agreement is however far from being excellent.

As the ASEP is expected to belong to the KPZ universality class, the scaling function of Section 4 should be observable in a large class of systems (growing interfaces, directed polymers in $1+1$ dimension, noisy Burgers equation). It would be worth to try on other growth models such as the RSOS,[13] the Eden model,[14] or polynuclear growth models.[15, 16]

As in ref. 5, we have considered here the large deviation function for a finite system in the long time limit (in technical words, we have calculated the largest eigenvalue of the matrix $M(\alpha)$). This means that we take the limit $t \to \infty$ first, and then we take the limit of a large system. This makes difficult the direct comparison with the results of simulations which were done, in particular for directed polymers, in an infinite geometry (so where the limits $t \to \infty$ and $N \to \infty$ were exchanged).[1, 17–19] It is interesting to note however that, though the order of limits is interchanged, our predictions of Section 4 for the tails of the large deviation function in the scaling region agree with the numerical results done in the infinite geometry,[17] with a similar non-gaussian shape i.e. $f(v) \sim -|v|^{3/2}$ on one side and $f(v) \sim -|v|^{5/2}$ on the other side (Note that for the infinite system, the $f(v) \sim -|v|^{3/2}$ tail can also be understood from replica calculations[20] or from heuristic arguments[16]). The structure of the large deviation function for finite times may thus not be so different from the one found in the present paper in the infinite time limit. Note that the calculation at finite time would imply a calculation including the contribution of all the eigenvalues, similar to the thermodynamic Bethe ansatz.[21]

APPENDIX A: BETHE ANSATZ EQUATIONS

In this appendix, we calculate the largest eigenvalue of the matrix $M(\alpha) = M_0 + e^{\alpha} M_1$ using the Bethe ansatz.[5, 11, 12, 22, 23]

A configuration $\mathscr{C}$ of the particles on the ring can be characterized by the p positions of particles, $1 \leqslant x_1 < x_2 < \cdots < x_p \leqslant N$. In the Bethe Ansatz, we choose a function of the form

$$\Psi(x_1, x_2, ..., x_p) = \sum_{Q} \mathscr{A}(Q) \prod_{k=1}^{p} [z_{q_k}]^{x_k} \tag{A1}$$

for $0 \leqslant x_1 \leqslant x_2 \leqslant \cdots \leqslant x_p \leqslant N$, where the sum is taken over all the possible permutations $Q = (q_1, q_2, ..., q_p)$ of the first p integers. We then try to determine the amplitudes $\mathscr{A}(Q)$ and the wavenumbers z_k for (A1) to give an eigenvector of the matrix $M(\alpha)$ when $1 \leqslant x_1 < x_2 < \cdots < x_p \leqslant N$

$$\lambda(\alpha)\ \Psi(\mathscr{C}) = \sum_{\mathscr{C}'} M(\mathscr{C}, \mathscr{C}')\ \Psi(\mathscr{C}') \tag{A2}$$

For configurations $\mathscr{C}$ where no particles are nearest neighbors, (A2) becomes

$$\lambda(\alpha)\ \Psi(x_1, x_2,..., x_p) = -p\Psi(x_1, x_2,..., x_p) + e^{\alpha} \sum_{j=1}^{p} \Psi(x_1,..., x_j - 1,..., x_p) \tag{A3}$$

(we exclude, for the moment, the case $x_1 = 1$ to avoid dealing with boundary conditions). Using (A1), the sum gives

$$\sum_{j=1}^{p} \Psi(x_1,..., x_j - 1,..., x_p) = \Psi(x_1, x_2,..., x_p) \left(\sum_{j=1}^{p} \frac{1}{z_j} \right) \tag{A4}$$

and (A3) becomes

$$\lambda(\alpha) = -p + e^{\alpha} \left(\sum_{j=1}^{p} \frac{1}{z_j} \right) \tag{A5}$$

We now consider configurations $\mathscr{C}$ where only two particles j_0 and $j_0 + 1$ are nearest neighbors, i.e., $x_{j_0+1} = x_{j_0} + 1$. Equation (A2) becomes

$$\lambda(\alpha)\ \Psi(x_1, x_2,..., x_p) = -(p-1)\ \Psi(x_1, x_2,..., x_p) + e^{\alpha} \sum_{\substack{j=1 \\ j \neq j_0+1}}^{p} \Psi(x_1,..., x_j - 1,..., x_p) \tag{A6}$$

meaning that all particles can move except the one in x_{j_0}. Using the expression (A5) of $\lambda(\alpha)$ and (A4) yields

$$e^{\alpha}\Psi(x_1,.., x_{j_0}, x_{j_0},..., x_p) = \Psi(x_1, x_2,..., x_{j_0}, x_{j_0} + 1,..., x_p) \tag{A7}$$

or, replacing Ψ by its expression (A1),

$$\sum_{Q} \mathscr{A}(Q) \left(\frac{e^{\alpha}}{z_{q_{j_0+1}}} - 1 \right) \prod_{k=1}^{p} (z_{q_k})^{x_k} = 0 \tag{A8}$$

where we have used that $x_{j_0+1} = x_{j_0} + 1$. The products $\prod_{k=1}^{p} (z_{q_k})^{x_k}$ for different permutations Q are independent functions of the x_k's except when the permutations differ only in the exchange of q_{j_0} and q_{j_0+1} (because x_{j_0} and x_{j_0+1} are not independent). We write that the coefficient in front of

each independent function vanishes in (A8) and find that for any $q_1, q_2, ..., q_p$,

$$\frac{\mathscr{A}(q_1, ..., q_{j_0+1}, q_{j_0}, ..., q_p)}{\mathscr{A}(q_1, ..., q_{j_0}, q_{j_0+1}, ..., q_p)} = -\frac{e^{\alpha} - z_{q_{j_0+1}}}{e^{\alpha} - z_{q_{j_0}}} \tag{A9}$$

Successive uses of (A9) lead to a first relation between $\mathscr{A}(q_1, q_2, ..., q_p)$ and $\mathscr{A}(q_2, ..., q_p, q_1)$

$$\frac{\mathscr{A}(q_1, q_2, ..., q_p)}{\mathscr{A}(q_2, ..., q_p, q_1)} = (1-)^{(p-1)}(e^{\alpha} - z_{q_1})^{(p-1)} \prod_{k=2}^{p} (e^{\alpha} - z_{q_k})^{-1} \tag{A10}$$

Due to periodic boundary conditions, the relation

$$\Psi(0, x_2, ..., x_p) = \Psi(x_2, ..., x_p, N) \tag{A11}$$

has to be satisfied for (A1) to be a solution of (A2) even when $x_1 = 1$. This leads to another independent relation between the $\mathscr{A}(q_1, q_2, ..., q_p)$ and $\mathscr{A}(q_2, ..., q_p, q_1)$

$$\mathscr{A}(q_1, q_2, ..., q_p) = z_{q_1}^N \mathscr{A}(q_2, ..., q_p, q_1) \tag{A12}$$

Combining (A12) with (A10) finally gives the Bethe Ansatz equations

$$z_j^{-N}(e^{\alpha} - z_j)^p = (-1)^{(p-1)} \prod_{k=1}^{p} (e^{\alpha} - z_k) \tag{A13}$$

that the z_j should satisfy for (A1) to be an eigenvector of $M(\alpha)$.

If we make the change of variables $y_j = (z_j e^{-\alpha} - 1)$, equation (A13) reduces to (8)

$$(1 + y_j)^{-N} y_j^p = e^{\alpha N}(-1)^{(p-1)} \prod_{k=1}^{p} y_k \tag{A14}$$

and the expression $\lambda_{\max}(\alpha)$ becomes

$$\lambda(\alpha) = -\sum_{j=1}^{p} \frac{y_j}{1 + y_j} \tag{A15}$$

where the $\{y_j\}_{1 \leqslant j \leqslant p}$ is a solution of the p equations (A14).

APPENDIX B: CALCULATION OF $\lambda_{\max}(\alpha)$

In this appendix, we establish expressions (14, 15) and (27, 28) of $\lambda_{\max}$ as a function of α, for the two choices (13) and (26).

Derivation of (14)–(15)

First we consider choice (13). Let y_j be the solution of

$$y_j = B^{1/p} e^{2i\pi j/p} (1 + y_j)^{N/p} \tag{B1}$$

which vanishes as $B \to 0$. For any function $g(y)$ analytic in the neighborhood of $y = 0$, $g(y_j)$ can be written, using Cauchy's theorem, as

$$g(y_j) = \frac{1}{2\pi i} \oint dy \left[1 - \frac{Ny}{p(1+y)} \right] \frac{1}{y - B^{1/p} e^{2i\pi j/p} (1+y)^{N/p}} g(y) \tag{B2}$$

where the contour surrounds the single root y_j of (B1). For small $|B|$, we can choose for the contour a circle of radius ε, with $|B|^{1/p} \ll \varepsilon \ll 1$, centered in $y = 0$.

Thus the contribution of y_j to λ in (9) is

$$\frac{-y_j}{1+y_j} = -\frac{1}{2\pi i} \oint dy \left[\frac{y}{1+y} - \frac{Ny^2}{p(1+y)^2} \right] \frac{1}{y - B^{1/p} e^{2i\pi j/p} (1+y)^{N/p}} \tag{B3}$$

We expand the integrand in powers of $B^{1/p}$ for small B and for each term in the expansion, we perform the integral over y. This gives

$$\frac{-y_j}{1+y_j} = \left(1 - \frac{N}{p} \right) \sum_{k=1}^{\infty} (B^{1/p} e^{2i\pi j/p})^k \frac{\Gamma((Nk/p) - 1)}{(k-1)!\, \Gamma((Nk/p) - k + 1)} \tag{B4}$$

When we sum, as in (9), over the p roots y_j, (i.e. over j for $1 \leqslant j \leqslant p$), all the terms for which k is not a multiple of p vanish and the non-vanishing terms of the form $k = pq$ give

$$\lambda_{\max}(\alpha) = -p \sum_{q=1}^{\infty} B^q \frac{(Nq-2)!}{(pq)!\, (Nq - pq - 1)!} \tag{B5}$$

which is (14).

The expression of y_j itself can also be obtained from (B2) in the same way, using $g(y) = y$,

$$y_j = \sum_{k=1}^{\infty} (B^{1/p} e^{2i\pi j/p})^k \frac{\Gamma((Nk/p) + 1)}{k!\, \Gamma((Nk/p) - k + 2)} \tag{B6}$$

To calculate α with the same method, we transform (12) in order to avoid that the contour of integration would cross the branch cut of the logarithm. From (B1), it is easy to see that

$$\prod_{j=1}^{p} y_j = (-1)^{p-1} B \prod_{j=1}^{p} (1+y_j)^{N/p}$$

and (12) becomes

$$\alpha = -\frac{1}{p} \sum_{j=1}^{p} \ln(1+y_j) \tag{B7}$$

Now the contribution of each root y_j in (B7) can be calculated using (B2) for $g(y) = \ln(1+y)$

$$\ln(1+y_j) = \frac{1}{2\pi i} \oint dy \left[1 - \frac{Ny}{p(1+y)} \right] \frac{1}{y - B^{1/p} e^{2i\pi j/p} (1+y)^{N/p}} \ln(1+y) \tag{B8}$$

Expanding again in powers of $B^{1/p}$, the coefficient of $B^{k/p}$ is

$$-\frac{1}{k} \ln(1+y) \frac{d}{dy} [(1+y)^{Nk/p} y^{-k}]$$

and the integral over y can be done easily by integration by parts. The rest is exactly the same as in (B4) and one finds

$$\ln(1+y_j) = \sum_{k=1}^{\infty} (B^{1/p} e^{2i\pi j/p})^k \frac{\Gamma(Nk/p)}{k!\, \Gamma((Nk/p) - k + 1)} \tag{B9}$$

After summation over j as in (B7), we obtain

$$\alpha = -\sum_{q=1}^{\infty} B^q \frac{(Nq-1)!}{(pq)!\, (Nq-pq)!} \tag{B10}$$

which is (15).

Derivation of (27), (28)

Let us now consider the case of large negative B, when the solutions of (10) are selected as in (26) in the limit $B \to -\infty$. If we make the change of variable

$$y_j = -1 - x_j \tag{B11}$$

the solution y_j of (10) we have selected in (26) becomes the solution of

$$x_j = D_j(1+x_j)^{p/N} \tag{B12}$$

where

$$D_j = -|B|^{-1/N} e^{i\pi(p+1-2j)/N} \tag{B13}$$

Equation (B12) is identical to (B1) (up to a change of notations) and we can proceed as in the small B case. For any function $g(x)$ analytic around $x=0$, one can write $g(x_j)$ as

$$g(x_j) = \frac{1}{2\pi i} \oint dx \left[1 - \frac{px}{N(1+x)} \right] \frac{1}{x - D_j(1+x)^{p/N}} g(x) \tag{B14}$$

when x_j is the solution of (B12) the closest to zero (here also the integration contour is small enough around $x=0$ to encircle only x_j).

In terms of the x_j, the expression (9) of λ becomes

$$\lambda = -\sum_{j=1}^{p} \frac{1+x_j}{x_j} \tag{B15}$$

As the function $g(x) = -(1+x)/x$ has a pole at $x=0$, expression (B14) has to be slightly modified (the contribution of the pole at $x=0$ has to be removed) and one can show that

$$-\frac{1+x_j}{x_j} = -\frac{1}{D_j} - \frac{1}{2\pi i} \oint \left[\frac{1+x}{x} - \frac{p}{N} \right] \frac{dx}{x - D_j(1+x)^{p/N}} \tag{B16}$$

After expanding in powers of D_j and integrating over x one gets

$$-\frac{1+x_j}{x_j} = -\left(1 - \frac{p}{N}\right) \sum_{k=-1}^{\infty} (D_j)^k \frac{\Gamma((pk/N)+1)}{(k+1)!\,\Gamma((pk/N)-k+1)} \tag{B17}$$

or by replacing D_j by its expression (B13)

$$-\frac{1+x_j}{x_j} = -\left(1 - \frac{p}{N}\right) \sum_{k=-1}^{\infty} \frac{\Gamma((pk/N)+1)}{(k+1)!\,\Gamma((pk/N)-k+1)} \times |B|^{-k/N} (-1)^k e^{i\pi(p+1-2j)\,k/N} \tag{B18}$$

Summing (B18) over the p roots selected in (26), as in (B15), yields

$$\lambda_{\max} = -\left(1-\frac{p}{N}\right) \sum_{k=-1}^{\infty} \frac{\Gamma((pk/N)+1)}{(k+1)!\,\Gamma((pk/N)-k+1)} |B|^{-k/N} (-1)^k \frac{\sin(pk\pi/N)}{\sin(k\pi/N)} \tag{B19}$$

which is (27).

Using $g(x) = x$ in (B14) gives also the expression of x_j itself and leads to

$$y_j = -1 - \sum_{k=1}^{\infty} \frac{1}{k!} \frac{\Gamma((pk/N)+1)}{\Gamma((pk/N)-k+2)} \left|\frac{1}{B}\right|^{k/N} (-)^k e^{((p+1-2j)\,ik\pi)/N} \tag{B20}$$

To calculate α, we use the change of variable (B11) in (12)

$$\alpha = \frac{1}{N} \ln |B| - \frac{1}{N} \sum_{j=1}^{p} \ln(1+x_j) \tag{B21}$$

The contribution of x_j is obtained from (B14), as in (B8)

$$\ln(1+x_j) = \sum_{k=1}^{\infty} \frac{\Gamma(pk/N)}{k!\,\Gamma((pk/N)-k+1)} (D_j)^k \tag{B22}$$

Again, we sum over the p leftmost roots x_j and find

$$\alpha = \frac{1}{N} \ln |B| - \frac{1}{N} \sum_{k=1}^{\infty} \frac{\Gamma(pk/N)}{k!\,\Gamma((pk/N)-k+1)} |B|^{-k/N} (-1)^k \frac{\sin((pk/N)\,\pi)}{\sin(k\pi/N)} \tag{B23}$$

which is (28).

Justification of (26)

To justify that choice (26) does give the largest eigenvalue of $M(\alpha)$ we are going to show that the p roots obtained from (26) coincide when $B \to -B_c$ with the p roots of choice (13). To do so, we take the logarithm of equation (10). If we define the logarithm $\ln y$ with a branch cut along $[0, +\infty[$, such that

$$\ln y = \ln |y| + i\phi \qquad \text{with} \qquad 0 \leqslant \phi < 2\pi$$

and $\ln(1+y)$ with a branch cut along $]-\infty, -1]$

$$\ln(1+y) = \ln|1+y| + i\phi \qquad \text{with} \qquad -\pi \leqslant \phi < \pi$$

the logarithm of (10), for negative B, becomes

$$p \ln y_j = \ln|B| + N \ln(1+y_j) + (2k_j - 1)\, i\pi \tag{B24}$$

Each root y_j corresponds to a value of the integer k_j. As B varies from $-\infty$ to 0, each root y_j of (10) changes continuously and the associated integer value k_j remains constant.

When $-B_c < B < 0$, each root y_j of choice (13) corresponds to

$$k_j = j \qquad \text{with} \quad 1 \leqslant j \leqslant p \tag{B25}$$

in (B24) whereas the $N-p$ roots which were excluded from choice (13) are given for small negative B by

$$y_l \simeq |B|^{-1/(N-p)}\, e^{(2l-1)\, i\pi/(N-p)} + \cdots \qquad \text{for} \quad 1 \leqslant l \leqslant N-p$$

and thus correspond to

$$k_l = \begin{cases} 1-l & \text{for} \quad 1 \leqslant l < (N-p+1)/2 \\ N+1-l & \text{for} \quad (N-p+1)/2 \leqslant l \leqslant N-p \end{cases} \tag{B26}$$

in (B24).

For large negative B, the N roots of (10) are of the form (26)

$$y_j \simeq -1 + |B|^{-1/N}\, e^{i\pi(p+1-2j)/N} \tag{B27}$$

and the corresponding value of k_j

$$k_j = \begin{cases} j & \text{for} \quad 1 \leqslant j \leqslant (N+p+1)/2 \\ j-N & \text{for} \quad (N+p+1)/2 < j \leqslant N \end{cases} \tag{B28}$$

We see by comparing (B25), (B26), (B28) that the roots selected in (13) for $-B_c < B < 0$ coincide with those selected in (26) for $-\infty < B < -B_c$. This proves that the expression (B6) of y_j for $-B_c < B < 0$ obtained using (13)

$$y_j = \sum_{k=1}^{\infty} \frac{1}{k!} \frac{\Gamma((Nk/p)+1)}{\Gamma((Nk/p)-k+2)} |B|^{k/p}\, e^{((2j-1)\, ik\pi)/p} \tag{B29}$$

coincides when $B = -B_c$ with the expression (B20)

$$y_j = -1 - \sum_{k=1}^{\infty} \frac{1}{k!} \frac{\Gamma((Nk/p)+1)}{\Gamma((Nk/p)-k+2)} \left|\frac{1}{B}\right|^{k/N} (-)^k e^{((p+1-2j)\, ik\pi)/N} \quad \text{(B30)}$$

derived from (26) for $B < -B_c$. (However, we note that by a direct comparison, it does not look obvious that (B29) and (B30) coincide, as they should for $B = -B_c$)

ACKNOWLEDGMENTS

We thank V. Hakim, J. L. Lebowitz, V. Pasquier and E. R. Speer for useful discussions

REFERENCES

1. T. Halpin-Healy and Y. C. Zhang, Kinetic roughening phenomena, stochastic growth, directed polymers and all that, *Phys. Rep.* **254**:216 (1995).
2. M. Kardar, G. Parisi, and Y.-C. Zhang, Dynamic scaling of growing interfaces, *Phys. Rev. Lett.* **56**:889 (1986).
3. A. L. Barabási and H. E. Stanley, *Fractal Concepts in Surface Growth* (Cambridge University Press, 1995).
4. F. Family and T. Vicsek, *Dynamics of Fractal Surfaces* (World Scientific, Singapore, 1991).
5. B. Derrida and J. L. Lebowitz, Exact large deviation function in the asymmetric exclusion process, *Phys. Rev. Lett.* **80**:209 (1998).
6. P. Meakin, P. Ramanlal, L. M. Sander, and R. C. Ball, Ballistic deposition on surfaces, *Phys. Rev. A* **34**:5091 (1986).
7. L. H. Tang, Waiting time formulation of surface growth and mapping to directed polymers in a random medium, in *Growth Patterns in Physical Sciences and Biology*, E. Louis, S. M. Sander, P. Meakin, and J. M. Garcia-Ruiz, eds. (Plenum, New York, 1992).
8. B. Derrida and M. R. Evans, The asymmetric exclusion model: exact results through a matrix approach, in *Nonequilibrium Statistical Mechanics in One Dimension*, V. Privman, ed. (Cambridge University Press, 1997), p. 277.
9. F. R. Gantmacher, *The Theory of Matrices*, *Vol. 2* (New York, Chelsea Pub. Co., 1959).
10. J. Krug, Origins of scale invariance in growth processes, *Adv. Phys.* **46**:139 (1997).
11. L.-H. Gwa and H. Spohn, Six-vertex model, roughened surfaces, and an asymmetric spin Hamiltonian, *Phys. Rev. Lett.* **68**:725 (1992).
12. L.-H. Gwa and H. Spohn, Bethe solution for the dynamical-scaling exponent of the noisy Burgers equation, *Phys. Rev. A* **46**:844 (1992).
13. J. M. Kim and J. M. Kosterlitz, Growth in a restricted solid-on-solid model, *Phys. Rev. Lett.* **62**:2289 (1989).
14. J. Kertész and D. E. Wolf, Noise reduction in Eden models: II. Surface structure and intrinsic width, *J. Phys. A* **21**:747 (1988).
15. J. Krug and H. Spohn, Anomalous fluctuations in the driven and damped Sine-Gordon chain, *Europhys. Lett.* **8**:219 (1989).

16. E. Ben-Naim, A. R. Bishop, I. Daruka, and P. L. Krapivsky, Mean-field theory of polynuclear surface growth, *J. Phys. A. Math. Gen.* **31**:5001 (1998).
17. J. M. Kim, M. A. Moore, and A. J. Bray, Zero-temperature directed polymers in a random potential, *Phys. Rev. A* **44**:2345 (1991).
18. T. Halpin-Healy, Directed polymers in random media: Probability distributions, *Phys. Rev. A* **44**:R3415 (1991).
19. J. Krug, P. Meakin and T. Halpin-Healy, Amplitude universality for driven interfaces and directed polymers in random media, *Phys. Rev. A* **45**:638 (1992).
20. Y. C. Zhang, Directed polymers in Hartree-Fock approximation, *J. Stat. Phys.* **57**:1123 (1989).
21. C. N. Yang and C. P. Yang, Thermodynamics of a one-dimensional system of Bosons with repulsive Delta-function interaction, *J. Mach. Phys.* **10**:1115 (1969).
22. D. Kim, Bethe ansatz solution for crossover scaling functions of the asymmetric XYZ chain and the Kardar–Parisi–Zhang-type growth model, *Phys. Rev. E* **52**:3512 (1995).
23. D. Kim, Asymmetrix XYZ chain at the antiferromagnetic transition: Spectra and partition functions, *J. Phys. A* **30**:3817 (1997).